

Contents lists available at ScienceDirect

Chemical Engineering & Processing: Process Intensification

journal homepage: www.elsevier.com/locate/cep



Treatment of textile wastewater by a hybrid ultrafiltration/electrodialysis process



Ridha Lafi^{a,*}, Lassaad Gzara^b, Ramzi Hadj Lajimi^c, Amor Hafiane^a

- ^a Laboratory of Water, Membrane and Environmental Biotechnologies, CERTE, BP 273, Soliman 8020, Tunisia
- b Center of Excellence in Desalination Technology, King Abdulaziz University, PB 80200, Jeddah 21589, Saudi Arabia
- ^c Department of Chemistry, College of Science, University of Hail, P.O. Box 2440, Hail 81451, Saudi Arabia

ARTICLE INFO

Keywords: Membrane Textile wastewater Ultrafiltration Electrodialysis

ABSTRACT

Conventional treatment of textile wastewater is generally based on physical-chemical treatment. Although the effluents from this can be discharged directly there is an increasing interest in industrial wastewater reuse. The present study is based on the investigation of the performance of a hybrid ultrafiltration/electrodialysis process for the removal of COD, salt, and color. Effects of temperature and intrinsic resistances were analyzed to study the ultrafiltration process. The ultrafiltration process was then integrated with electrodialysis (ED) for the treatment of Primary treated textile wastewater (PTTW) and was found that the hybrid process was capable of promoting the quality of the treated textile wastewater. In case of treated textile by UF with a ceramic membrane, ED process was effectiveness where the removal efficiency of TDS and conductivity were 94.2, 97.1% respectively corresponds to conductivity value of 0.450 mS/Cm at 25 min. It is noticeable that primary treated textile wastewater with combined UF–ED techniques present very similar values for the same parameter as the ones presented by normal feed water.

1. Introduction

The textile industry is one of the largest consumers of water, dyes and various processing chemicals that are used during the various stages of textile processing. Subsequently, substantial quantities of effluents are generated, mostly consisting of spent or unutilized resources, which are not suitable for further usage. These effluents are likely to cause environmental problems if discharged without prior treatment. The wastewater obtained from the textile industry is usually rich in color, chemical oxygen demand (COD), complex chemicals, inorganic salts, total dissolved solids (TDS), pH, temperature, turbidity and salinity [1]. Among the various complex constituents present in textile wastewaters, the dyes can be inarguably considered as the most peremptory source of contamination. The direct discharge of the colored textile effluent into the freshwater bodies adversely affects the aesthetic merit, water transparency and dissolved oxygen content [2]. Consequently, the volume and composition of textile wastewater exhibit wide heterogeneity, owing to a number of factors, including the characteristic quality imparted to processed fabric, properties and chemical and physical characteristics of the applied dye, nature of special finishing if any specificity of the process, the equipment used, and the principles on which water use has been modeled [3].

Various treatment techniques are in use to mitigate the contaminant levels of textile wastewaters. However, these methods suffer from certain serious handicaps. For instance, biological processes [4], physicochemical methods, such as chlorination, coagulation-flocculation [5,6], adsorption [7] and advanced oxidation processes, such as, ozonation [8], Fenton treatments [9], electro-Fenton methods [10], photo-Fenton oxidation processes [11], and photocatalytic reaction [12], for complete degradation of the toxic textile wastewater components [13–15].

However, traditional treatment techniques suffer from a number of loopholes. The application of membrane-based processes in such cases can quite effectively surmount most of these drawbacks. Microfiltration has limited application in textile wastewater treatment because of its close resemblance to conventional crude filtration processes. Microfiltration membranes usually have pore sizes in the range 0.1–10 µm; separation through microfiltration is usually effected at a low-pressure differential within 2 bars. These features account for its restricted implementation in textile industry. It is mainly used for removal of particles suspension and colloidal dyes from exhausted dye bath and from discarded rinsing bath discharge; microfiltration membranes, however, permit the unconsumed auxiliary chemicals, dissolved organic pollutants and other soluble contaminants to escape with the permeate [16]. Ultrafiltration is a membrane separation process, mostly

E-mail address: ridha.lafi@yahoo.fr (R. Lafi).

^{*} Corresponding author.

used in the separation of macromolecules and colloids from a solution; solutes retained usually have molecular weights of a few thousand Daltons. The ultrafiltration membrane process has limited applications in the textile industry; this is mainly because the molecular weights of the dyes present in the highly colored textile discharge are much lower than the molecular weight cut-off (MWCO) of the ultrafiltration membranes [17]. Furthermore, recently, the potential of ceramic membranes as viable replacements of polymer membranes in the UF pretreatment step was investigated; the preference of ceramic membranes over ordinary polymer membranes was based on their exhibition of comparatively high permeability rates and several other advantageous properties they are endowed with, such as, high mechanical, chemical, and thermal stability [18]. Ceramic UF membranes performed very well in the treatment of pulp and paper mill wastewater, with turbidity and total suspended solids removal ratio above 99% [19], as well as in the disposal of textile wastewater with the removal of dye up to 95.2% [20]. Ultrafiltration (UF) is usually applied as a pre-treatment step in systems demanding a high degree of process stream purification; it is followed by processes such as nanofiltration (NF), or reverse osmosis (RO) stages, which satisfy the demands on process water quality [21,22].

Over recent years, water consumption, wastewater treatment, and the effluent reuse potential have become crucial factors for sustainable production. This has prompted studies on water reuse within the industrial sector [23] presented a multiple membrane separation processes, where UF and MF were used for pre-treatment; secondly, electrodialysis (ED) was carried out for effective desalination.

Electrodialysis (ED) is considered an electro-driven membrane process involving ion exchange membranes are not only a part of applied in electrochemistry but also belong to the field of separation techniques [24]. Compared to other kinds of membrane technologies, it uses an electrical current, rather than pressure, to induce the ions to pass through the membrane; the use of pressure is a major cost factor for other membrane processes. And also, it can be used a low level of electrical current, which helps to reduce the cost of ED. In addition, ED has attractive characteristics such as a high selectivity, a high product recovery ratio and can destroy at least some of the components in the raw water (drinking or waste), and it can run continuously. Yet, ED does not require treatment chemicals "green technology", and cost-effectiveness [25,26] all of these advantages may be pointed out to the utilize ED in the future as an effective technique. Sometimes it becomes necessary to use two or more methods of treatment, i.e., hybrid processes, to ensure effective treatment of wastewater [27,28]. However, based on literature reviews, so far no other studies have taken into account to the investigation of the integrated process (UF-ED) combining membrane technologies (ED) and ultrafiltration processes (UF) in the treatment of textile wastewater.

The main objective of this study is to investigate the applicability of integrated process using a combination of UF and ED in the treatment at the source of real primary treated Textile Wastewater (PTTW). UF is used for separation of the macromolecules and colloids and degradation of color. ED allows the ionic species separation. This approach can produce water suitable of process met reuse criteria with characteristics described in Table 1

Preliminary experiments were performed at a laboratory scale in order to evaluate the performance of each process and to investigate the experimental conditions for the electrodialysis process.

2. Materials and methods

2.1. Sampling

The general experimental flow sheet used in this work is presented in Fig. 1. The effluent of the current study was supplied from the discharge dyeing effluent of a textile factory specialized in the dyeing of cotton fabric and located in Ksar Hellal, Tunisia. Different dyes

Table 1Reference values for water reuse in textile industry.

Parameter	Criteria
COD (mg/L) Conductivity (µS/Cm) pH Turbidity (NTU) Color Suspended Solids (mg/L) Dissolved Solids (mg/L)	60–80 1000 6–8 1 None 5
Total Hardness (mg/L as CaCO ₃)	25–50

(reactive and direct), chemical substances such as detergents, salts, auxiliaries (e.g. surfactants, emulsifiers) and caustic soda are used in the factory dying process.

The generated wastewater is collected in a sewer system, which crosses throughout the factory. Then, this wastewater is directed to a pump station and then driven to a dynamic rotating screen. Fine particles have been removed; pH is lowered to 10 and equalized. The final stage consists of a biological reactor and later dissolved air flotation tank to separate the activated sludge from the final effluent. The resulting treated wastewater can be considered as a Primary Treated Textile Wastewater (PTTW) and can be considered also as the raw water for later UF/ED treatment processes. Wastewater samples have been collected after sludge removal and before chlorination. Wastewater samples were first filtered on a 0.45 μ m membrane before analysis. Primary treated textile wastewater (PTTW) characteristics are shown in Table 2.

2.2. Analytical methods

The wastewater analyses were carried out in accordance with the Standard Methods for Examination of Water and Wastewater [29]. pH, conductivity, COD, and color were determined with (A Jenway 3040 brand, HACH HQ40d, closed reflux titrimetric method 5220C, A-Analyst 400. Cations were analyzed by atomic absorption spectrometer AAS Vario 6 Spectrometer. Chloride and Sulphate were quantified by argentometric and gravimetric method respectively.

2.3. Membrane module UF and experimental procedure

The schematic of UF/MF pilot 50 CM2 was used in the experiments is shown in Fig. 2. For all experiments, we operated at constant Cross Flow Velocity (CFV = $6\,\text{m/s}$). The permeate was not recycled in the feed tank.

A membrane T170-50n TZ single channel tubular ceramic membrane was used to filter the colored solutions. The specifications of the membrane are given in Table 3.

Experiments were carried out under three different temperatures (20, 30, and 40 °C) in order to observe membrane performances at each temperature. The process performances were studied in terms of both, permeate flux and permeate quality.

After each UF run, the membrane was subjected to a cleaning cycle which included in the first place a rinse with deionized water at $25\,^{\circ}\mathrm{C}$ (15 min). Next, an alkaline cleaning with aqueous NaOH solution (pH 13) at $60\,^{\circ}\mathrm{C}$ (1 h) took place. Finally, the membrane was rinsed with deionized water until neutrality. The cleaning procedure after runs with the feed concentration included an additional step since alkaline cleaning was not enough to recover the initial permeability. It consisted of an acid cleaning step with the aqueous citric acid solution (pH 2) at $40\,^{\circ}\mathrm{C}$ (1 h), followed by rinsing with deionized water until neutrality was reached. All the cleaning steps, including rinses, were conducted at a CFV of $3\,\mathrm{m/s}$ and no pressure was applied. Once the membrane was cleaned, the water permeability was checked. The mentioned cleaning process allowed initial flux recoveries higher than 90%.

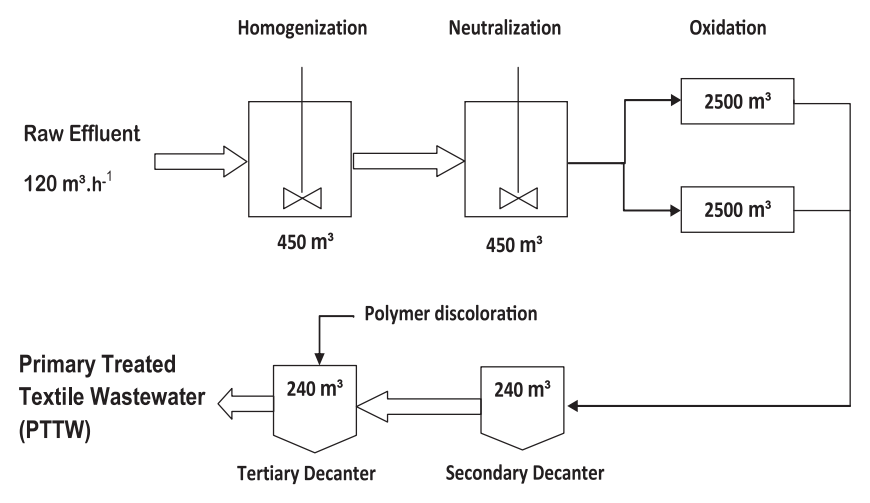


Fig. 1. The schematic of wastewater treatment plant.

 Table 2

 Characteristics of primary treated textile wastewater (PTTW) and UF permeate.

	PTTW	Permeate UF
pН	8.6	8.6
Turbidity (NTU)	7.8	0.54
Conductivity (mS/Cm)	7850	4520
Na ⁺ (mg/L)	2046	1974
K ⁺ (mg/L)	98	86
Ca ²⁺ (mg/L)	27	22
Mg^{2+} (mg/L)	17	10
Cl (mg/L)	602	552
SO ₄ ²⁻ (mg/L)	830	802
HCO ₃ (mg/L)	3610	3420
TDS (mg/L)	2980	2400
COD, mg O ₂ /L	220	100

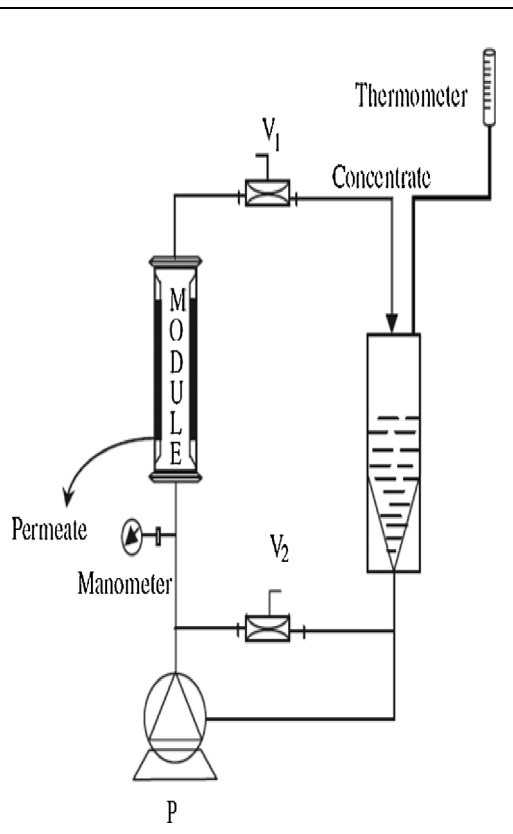


Fig. 2. The schematic of UF/MF pilot 50 CM2.

Table 3Ceramic membrane specifications.

Membrane	T170-50n TZ
Туре	Tubular
Active layer	ZrO_2
Nominal pore size	50 nm
Deionized water permeability	
Length	254 mm
Outside diameter	10 mm
Internal diameter	7 mm
Effective filtration area	50 cm ²
Maximum operating temperature	95 °C
Maximum operating pressure	5 bar
pH range	0–14

The permeate flux is calculated according to Eq. (1)

$$J_p = \frac{V}{At} \tag{1}$$

where J_p is the permeate flux (L/m²h), V is the permeate volume (L), A is the effective membrane area (m²) and t is the sampling time (h). At the same time, permeate samples were collected for water quality analysis. The rejection coefficient (R) is calculated as a percentage according to Eq. (2)

$$R(\%) = \left(1 - \frac{C_p}{C_f}\right) \times 100 \tag{2}$$

where C_f is the concentration in the feed stream and C_p is the concentration in the permeate stream.

The volume reduction factor (VRF) is equal to the initial feed volume divided by the retentate volume:

$$VRF = \frac{V_f}{V_r} \tag{3}$$

Darcy's law is commonly used to determine filtration resistance in permeate transport through porous membranes according to Eq. (3)

$$J_p = \frac{\Delta P}{\mu R_t} \tag{4}$$

where J_p is the permeate flux (L h⁻¹ m⁻²), ΔP is the transmembrane pressure (Pa); μ is the dynamic viscosity of the feed (Pa s) and R_t is the total filtration resistance (m⁻¹).

Resistances in series models [30,31] of membrane fouling often subdivide the total membrane resistance $R_{\rm t}$ into three components, namely intrinsic membrane resistance $R_{\rm m}$, external (concentration polarization) resistance $R_{\rm cp}$; and internal resistance $R_{\rm f}$, due to fouling.

Table 4 Characteristics of ion-exchange membranes.

Membrane type	Anion exchange membrane PC–SA	Cation exchange membrane PC–SK
Thickness (µm)	180-220	160-200
Perm selectivity	0.93	0.96
Functional groups	NH ₄ Cl	SO₃Na
Temperature stability, max (°C)	60	50
Chemical stability (pH)	0–9	0–11
Ion exchange capacity (meq g ⁻¹)	≈1.5	≈1
Surface potential (Ω cm ²)	1-1.5	0.75-3
Transport number	> 0.96	> 0.93

2.4. Electrodialysis pilot and experimental set-up

The electrodialysis unit PCCell ED 64004 obtained from PCCell GmbH was utilized. In this work; two Cation exchange membrane (PC–SK) and one anion exchange membrane (PC–SA) was applied. Electrodialysis experiments were performed in a pilot-scale ED system, using platinized titanium (Titane/Pt-Ir coated) electrode as anode and cathode with the effective membrane area of 64 cm² per membrane, the distance between two membranes was 0.5 mm. During all experiments, conductivity, TDS of solution and cations and anions concentrations were recorded. The solution sodium sulfate at a concentration of 0.01 M was used as electrode rinsing solution in all experiments. The effluent was fed into the concentrate and dilutes chambers in the ED cell. Thus, the characteristics of ion exchange membranes used in the ED process were shown in Table 4. And also, Experimental setup of the ED process was shown in Fig. 3.

The permeate collected by Ultrafiltration for the applied pressure $2.05\,\mathrm{bar}$ and a temperature of $20\,^\circ\mathrm{C}$ was used as feed for all the ED system. This pre-treatment step was obtained a clear permeate by removing organic matters.

During the experiments for ED, the volume of dilute, concentrate, and the same solution was used. Prior to the experiments, $0.1~\rm M~Na_2SO_4$ was used as electrode rinse solution circulating in electrode compartments, in order to prevent the generation of chlorine or hypochlorite, which could be hazardous for the electrodes. The flow rate of the electrode rinse solution was fixed to $40~\rm L/h$ for all experiments. Although the flow rate of other solutions (dilute and concentrate) were fixed at the beginning of the experiment. Dilute and concentrate were recirculated through the ED cell at these flow rates until the desired product concentration or TDS ($<0.5~\rm g/L$) was achieved in the dilute.

The efficiency of the UF–ED integrated system was evaluated by comparing analysis values of the effluent before and after treatment. Besides that, the performance of the UF–ED treatment was also monitored to evaluate the influence of using recycled water for effluent discharge standards.

2.5. Determination of the demineralization rate

The conductivity allowed following the demineralization rate [32,33]. The demineralization rate can be calculated as

$$DR(\%) = 100(1 - \frac{EC_0}{EC_t})$$
 (5)

where DR is the demineralization rate expressed in percentage, EC_0 and EC_t are, respectively, the initial and conductivity of the dilute, expressed in μS cm $^{-1}$.

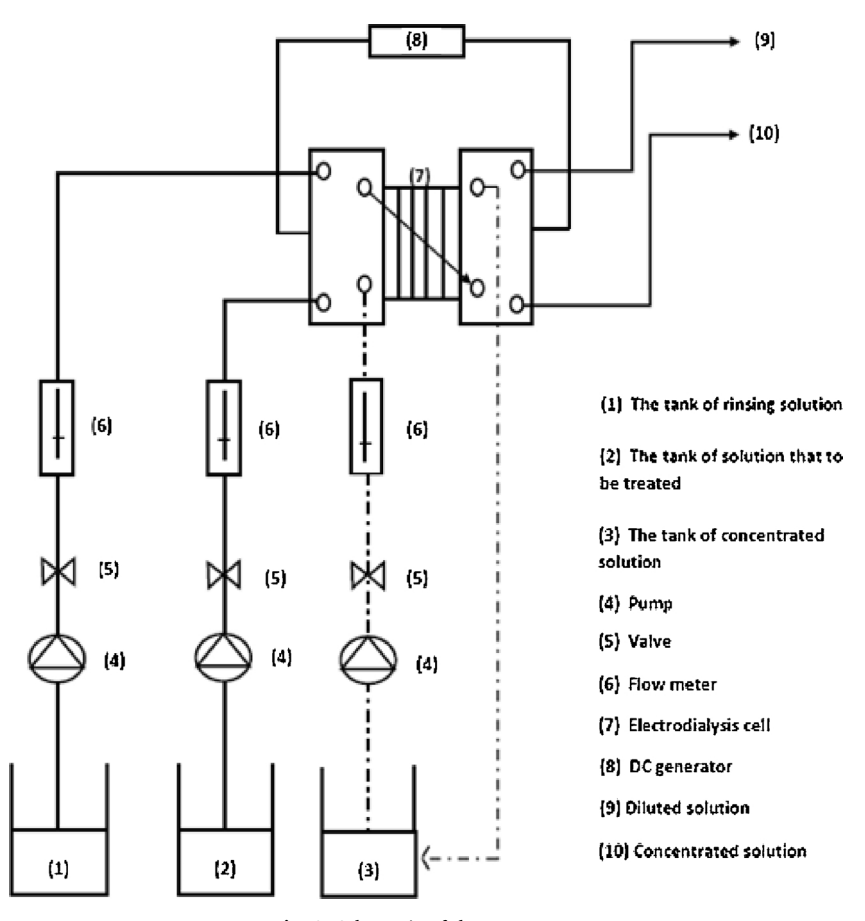


Fig. 3. Schematic of the ED system.

2.6. Determination of limiting current (Ilim)

The applied current density across the ED cell was fixed at a value below the limiting current (I_{lim}) which is determined by primary tests. The limiting current can be determined experimentally by plotting the electrical resistance across the membrane stack or the potential value in the dilute cell as a function of the reciprocal electric current (I^{-1}). This is called a Cowan–Brown plot after its original developers [34]. Permeate of UF was used to determine these values at different flow rates. The applied current in all experiment was fixed from the beginning to a value below the limiting current ($I = 0.8I_{lim}$).

2.7. Determination of energy consumption (EC)

Energy Consumption (EC) in ED is an important parameter from the economical point of view, as it can be described as the energy consumed for desalting one liter of feed solution [35]:

$$EC = \frac{E\int_0^t Idt}{V} \tag{6}$$

Where E is the applied potential, I the current, V the dilute stream volume and t is the time.

3. Results and discussion

3.1. Influence of operating conditions on permeate flux

3.1.1. Effect of TMP

The water membrane permeability was determined by measuring the permeate flux of deionized water at a different temperature and the CFV was set to 6 m/s. The deionized water flux of the ceramic membrane in all experiments is shown in Fig. 4, since the temperature effect on the filtration process, was investigated with the ceramic membranes; its hydraulic permeability was also measured at several temperatures. The values of water permeability obtained at 20, 30 and 40 $^{\circ}$ C were 222.9, 249.9, and 274.7 L/h m²bar, respectively. Therefore, a temperature increase leads to higher deionized water permeate flux due to an increase of the mass-transfer coefficient [36].

Fig. 4 illustrates permeate flux (J_p) as a function of TMP for the three temperatures studied at textile wastewater.

The values of J_p for textile wastewater conditions were lower than J_p initial values under any operating condition (Fig. 4), which indicates that there was a decrease in permeate flux during the experiments. As reported, permeate flux decline is a consequence of membrane fouling and might be due to several factors such as adsorption of organic pollutants onto the membrane surface and into the pores, concentration

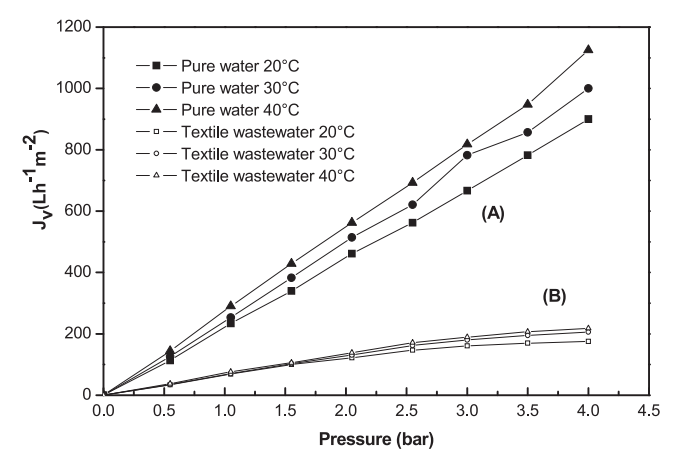


Fig. 4. Effect of TMP on permeate flux at different temperature for (A): Deionized water and (B): Textile wastewater.

polarization and cake layer formation [37]. The differences between deionized water and textile wastewater J_p values were more pronounced at higher TMP (at a fixed temperature of 20 °C, the flux reduction at 1 bar was 70% while at 4 bar was much higher, 80%), probably because under these conditions the convection of particles toward the membrane surface is enhanced [38] and thus, the accumulation of organic pollutants are more easily deposited onto the membrane surface or into the pores, increasing membrane fouling and leading to a major decrease of permeate flux.

Initially, permeate flux increased with an increase in operating pressure nearly corresponding to a linear equation, as expected, since TMP is the driving force of the UF process. Nevertheless, at textile wastewater conditions, when membrane fouling was likely to have occurred as a consequence of the different mechanisms previously stated, the trend was slightly different. For instance, at a fixed temperature of 20 °C, permeate flux increased by 43% as TMP was changed from 1 to 2 bars. By further increasing operating pressure, less significant improvement in textile wastewater permeate flux was obtained. This was observed at any temperature tested. Moreover, at TMP higher than 2.5 bar, permeate flux was independent of TMP. This could be attributed to the accumulation of solute particles near the membrane surface and the formation of a cake layer [39]. Textile wastewater in cross-flow membrane filtration is reached when the solute flux driven toward the membrane by convection is compensated by the back transport of the solute away from the membrane [40]. In this way, this filtration stage is characterized by a constant thickness of the cake layer. When feed pressure increases, a thicker and more compacted cake layer is obtained at the equilibrium state. By that, both the driving force of the filtration process and the filtration resistance are increasing. When these opposed effects are compensating each other, steady-state permeate flux is independent of TMP [41], and the process becomes mass transfer-controlled. Similar results are reported by Waeger et al. [42] using ceramic ultrafiltration membranes for particle removal from anaerobic digester effluent. As shown in Fig. 4 Increasing TMP up to 2.55 bar increases permeate flux; however, after that flux is nearly constant, so that it is necessary to work with a lower critical pressure around 2.55 bars.

3.1.2. Effect of temperature

The results obtained during experiments with textile wastewater showed that permeate flux decline from the beginning of the run to the steady-state condition was lower at the higher temperature (Fig. 4). In fact, as an example, for a fixed TMP of 4 bar, permeate flux decreased by 80.5% from its initial value when the operating temperature was set at 20 °C. Lower permeate flux decline as temperature increases is a consequence of the reduction of membrane fouling and concentration polarization under higher temperature.

The temperature of textile wastewater was controlled from 20 to 40 °C using a water bath. Fig. 5 Shows the variation of the permeate flux after 6 h of filtration at different feed temperatures. The permeate flux increases by 18% with increases of feed temperature from 20 to 40 °C. As seen, at a higher temperature cake layer formation is limited and permeate flux is almost constant [43]. It must be mentioned that by increasing temperature, permeate flux increases. Temperature has double effects on permeation flux; increasing temperature decreases viscosity, and as a result increases permeation flux [44,45]. From another point of view, increasing temperature increases osmotic pressure and this decreases permeation flux. Therefore, because of the bilateral effects of temperature must be specified. Higher feed temperature leads to lower viscosity of feed and also higher solubility of some feed constituents. The same reduces concentration polarization and transport of solvent through the membrane intensifies, yielding a higher permeates flux. It should be noted that the elevation of feed temperature normally increases the energy cost and the potential of scaling, and reduces the durability of the membrane system in spite of superior thermal stability of ceramic membrane compared to the polymeric membrane.

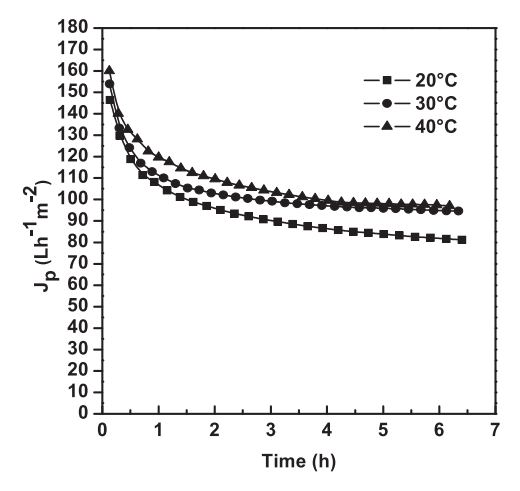


Fig. 5. Effect of temperature on permeate flux (CFV = 6 m/s, TMP = 2.05 bar).

The collected permeate under a TMP of 2.05 bar was used as feed for all the ED system. This pre-treatment step was obtained a clear permeate by removing organic matters.

The cumulative permeate volume Vp obtained as a function of time for the ceramic membrane at different temperature and with constant CFV = 6 m/s, is represented in Fig. 6. As it can be observed, these volumes increased with processing time, but simultaneously, a decrease occurred in the permeate rate. Additionally, for a given time, the volumes decreased with increased temperature. Fig. 6 also includes the cumulative permeate volume obtained in the previous experiments for the filtration of pure water with the ceramic membrane. The lower values of Vp obtained of textile wastewater in comparison to those of pure water were due to the fouling of the membrane [43]. It is also seen that there is a linear relationship between the permeate volume of pure water and time, which implies that J_p is constant. This is in accordance to the resistance in the series model, given by Darcy's law.

From the relation between VRF and filtration time, it is easy to deduce the influence of VRF for the experiments. Fig. 7 shows the effect of temperature on permeate flux decline, the flux increases with VRF increases, due to increasing fouling. Moreover, these curves could be divided into three periods: an initial stage with a rapid decrease of the permeate flux; a second stage with a smaller decrease of the permeate flux that takes place around VRF = 1.25 and a final stage with observed a constant flux after VRF = 1.25.

The results shows a constant permeate flux at $79.54 \, \text{L/h m}^{-2}$ of

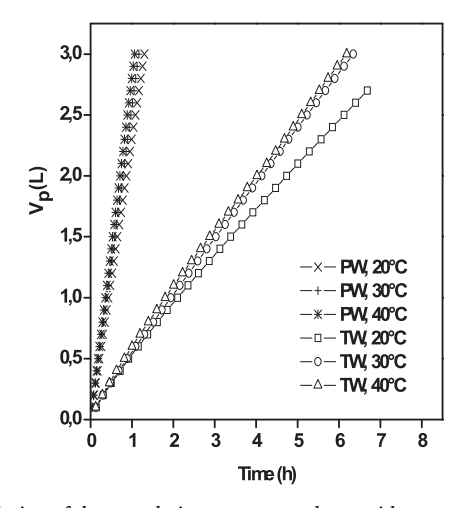


Fig. 6. Evolution of the cumulative permeate volume with processing time for the wastewater filtration with the ceramic membrane at a tangential velocity CFV = $6\,\text{m/s}$.

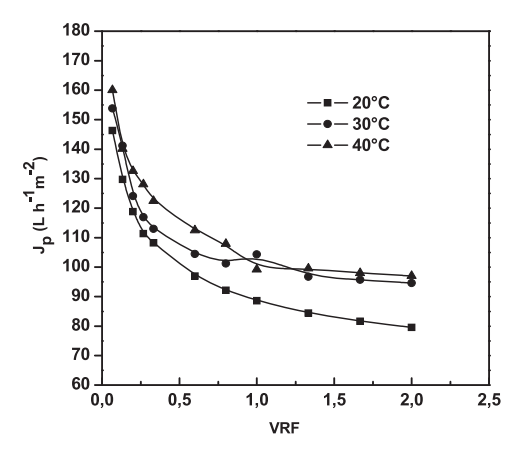


Fig. 7. Evolution of the permeate flux with the volume retention factor (CFV = $6\,m/s$, TMP = $2.05\,bar$).

VRF = 2–20 °C and 94.59 L/h m² of VRF = 2–30 and 40 °C. On operating temperatures 30 and 40 °C, it can be observed no influence on the permeate flux was noticed since an increase in the temperature, flux decline with VRF was practically negligible.

3.1.3. Analysis of resistances

Fig. 8 Illustrates the membrane fouling of ultrafiltration in treating textile wastewater at CFV = 6 m/s and TMP = 2.05 bar with different temperatures 20, 30 and 40 °C. R_m decreases with increasing temperature, due to lower values of the viscosity of the liquid, and because of the increase of the mass-transfer coefficient according to the film model, both effects providing higher pure water permeate flux at higher temperature. On the contrary, R_a increases with temperature, indicating more severe fouling phenomena at the higher temperature. As consequence, a temperature increase results first in a greater external fouling on the membrane surface probably due in an increment of the internal fouling due to adsorption and pore blocking. As filtration times progress, the adsorption resistance (Ra) increased. This increase due to high turbulence (CFV = 6 m/s) can cause the relatively smaller or finer particles. The finer particles present in textile wastewater are then deposited either in the membrane pore opening or into membrane pores channels [46].

3.2. Electrodialysis of PTTW treated by UF

3.2.1. Determination of limiting current density

The feed sample collected from ultrafiltration was circulated through the depleting compartments at three flows rate (10, 20 and

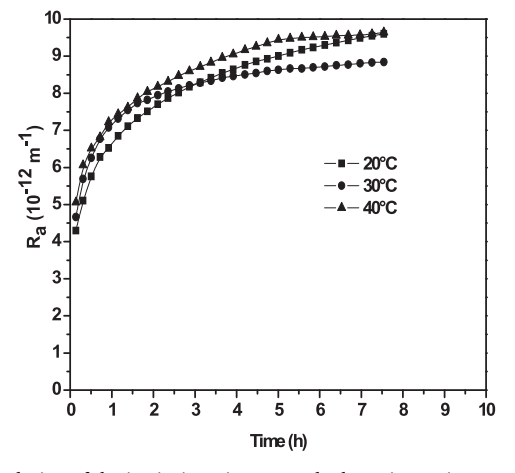


Fig. 8. Evolution of the intrinsic resistance and adsorption resistance with time at different temperatures (CFV = 6 m/s, TMP = 2.05 bar).

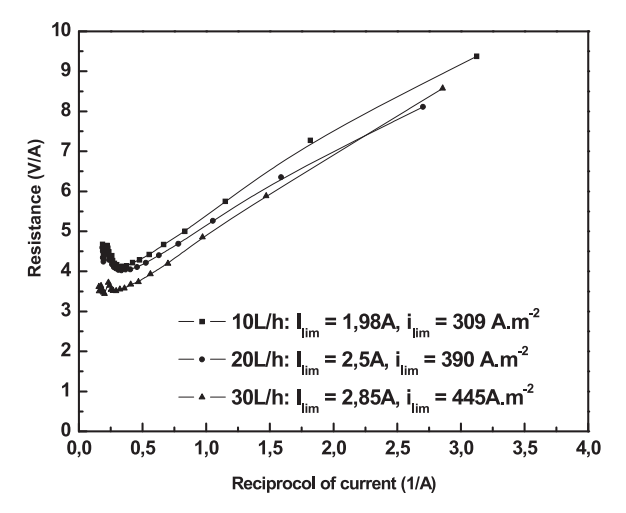


Fig. 9. Limiting current density determination curve.

30 L/h).

In this study, the limiting current ($I_{\rm lim}$) was determined by Cowan–Brown method by measuring the potential and the cell resistance as a function of the applied current. Fig. 9 shows the curves illustrating the determination of the limiting current from the experimental result obtained with a feed sample collected and a different flow rate. The limiting current was determined from the graph showing the cell resistance versus the reciprocal of the current. Firstly, the applied current (the limiting current) is depending on the flow rate, it is lower for low flow rate. Secondly, the experiment times to obtain the same results augmented by increasing the flow rate. It was not possible to increase the flow rate above 30 L/h since the maximum capacity of the pumps in the present system is defined as 30 L/h.

The applied current in all experiment was fixed from the beginning to a value below the limiting current $(I = 0.8I_{lim})$.

3.2.2. Effect of voltage

To study the effect of applied voltage, the concentration of feed solution is considered permeate of UF and the real inlet velocity was fixed at $10\,\mathrm{L/h}$.

Fig. 10 shows the variation of the output current in the system to the applied voltage between electrodes. There are three distinct parts of this curve

In the first part (I, E < 3 V), showed that in this region the resistance of the stack is relatively high. The applied voltage is not so

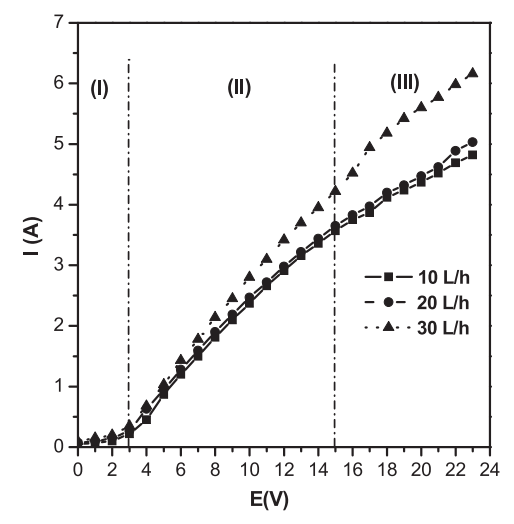


Fig. 10. Effect of applied voltage.

important to overcome the resistance of membranes and to induce the transport of several ions. At these conditions, there are few means of transports of ions between the dilute and concentrate compartments. In this region, the demineralization rate increases with an increase of the applied voltage, the demineralization rate only marginally with the increasing voltage drop. Consequently, low ionic fluxes are obtained in this region [47,48].

In the second part ($3 < E < 15 \, V$), a clear to increase in power is noticed. This current increases more or less linearly with the applied voltage which leads a more or less linear increase of the demineralization rate and ionic flux. In the same region, the resistance of the stack is quasi-constant and the current increased linearly with an increase of the applied voltage according to Ohm's law. The transport of ions between the compartments of the cell is proportional to current. These can explain the proportionality between demineralization rate, flux and the applied voltage [47].

In these two regions, the current efficiency is equal to the unit. All applied current is used for ions transport.

In the third part (E > 15 V), the current density increases linearly with increasing the applied voltage but with a less pronounced rhythm. The increase in the applied voltage does not lead to a significant increase in the demineralization rate and flux. At this point, the limiting current density is reached and there is no increase in the current density neither ionic transport from dilute to concentrate compartment when the applied voltage increases. Consequently, the reduction of current efficiency is noticed [47].

3.2.3. Conductivity and ions removal of PTTW treated by UF

In this study, textile wastewater treated by the UF process with the ceramic membrane was fed into the ED process. It can be seen from Fig. 11 the shift of ions was established at the first moment of the experiment. A sharp decreasing in textile wastewater conductivity from 4.5 to 1.2 mS/cm during the first 20 min was demonstrated. And also, it has decreased to 0.245 ms/Cm after 30 min. In the case of our experiments, this is anticipated as a result of a decrease in current as the conductivity is reduced but the removal efficiency of ions was increased. We notice that the DR decreases with an increase in the flow rate. This can be explained by the remaining time of ions inside the different compartments of the cell. In fact, the ions have more time to be transferred from one compartment to another though the membrane when the velocity or flow rate is lower.

The evolution with time of removal rate of demineralization of cations and anions in the treated water and for the flow rate $10\,L/h$ at applied voltage $10\,V$ is shown in Fig. 12. The removal efficiency of cations and anions it can be considered acceptable after $25\,\text{min}$. As shown in Table 5, it was clearly observed that the removal efficiency of TDS and conductivity were 94.2, 97.1% respectively. On the other

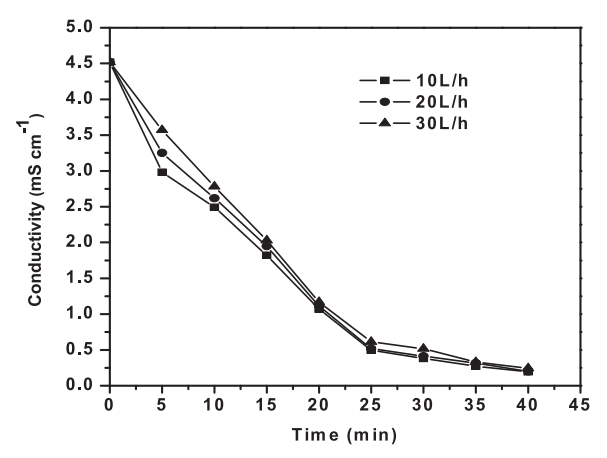
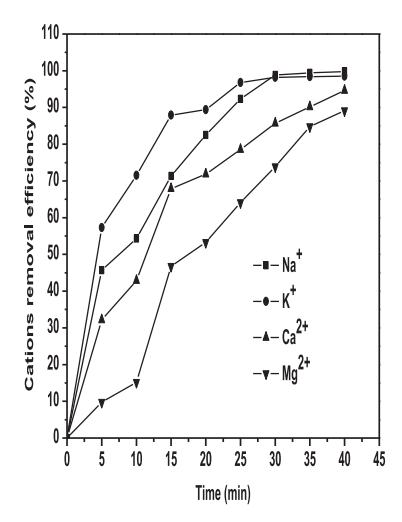


Fig. 11. Conductivity variations of PTTW treated by UF/ED.



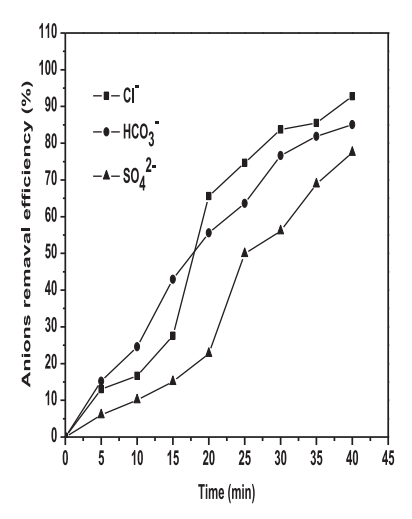


Fig. 12. Cations and anions removal efficiency with time by ED.

Table 5Composition of the primary treated textile wastewater by UF-ED.

Physico-chemistry parameter	After UF-ED separation
pH	5.3
Conductivity (mS/Cm)	0.45
TDS (mg/L)	210
COD (mg O ₂ /L)	50

words, it was also found that the effluent treated with combined UF-ED techniques provided water quality values very similar to values of feed water.

It is important to emphasize that the values obtained after UF–ED treatment for critical parameters like COD comply with present Tunisian legislation for effluent discharge standards as presented in Table 1. In relation to the reduction of organic compounds, UF has been shown to be a better option as well as for textile wastewater.

3.2.4. Desalination of the PTTW treated by UF/ED

Finally, the application of electrodialysis was performed on the real textile was tewater. Batch recirculation mode was adopted for this experiment. The flow rate and applied current were fixed respectively at $10\,\mathrm{L}\;\mathrm{h}^{-1}$ and 1.98 A. The experiment was achieved after 40 min.

As seen in Table 1, on the other words, it was also found that the primary textile wastewater treated with combined UF/ED techniques provided water quality values very similar to the values of feed water. In this experiment, the amount of specific power consumption was $0.9\,W\,h\,L^{-1}.$

3.3. Economical benefit

The water supply sources of textile factories in Ksar Helal industrial zone are municipal water with regard to the cost and water quality (1 $\rm m^3$ cost 0.980 DT). SITEX factory produces $120\,\rm m^3/h$ of raw effluent with a large amount of water that is highly colored, with high loading of the inorganic salt. In view of the decrease of the water consumption as well as the wastewater amount, water reuse using membranes is advisable [49]. The combined process of UF/ED membranes was applied for Primary Treated Textile Wastewater (PTTW), not only to improve the rejection efficiencies and flux recovery but also to recycle the permeate back into the process. The treated wastewater can be reused as refrigerating water, a washing water, and a process water.

4. Conclusion

The application of an integrated UF–ED process of textile wastewater was found to be effective. The efficiency in degrading organic matter by the UF process was proved by a significant reduction in COD. This pretreatment makes it possible to treat the effluent so that it then does not clog the membranes during ED. The results show significant reductions in all parameters tested. Comparing the values of the effluent treated with the association of UF–ED techniques to the values of usual feed water, the concentration in the permeate was under the detection limits, thus the quality of the UF–ED process met reuse criteria.

References

- A.K. Verma, R.R. Dash, P. Bhunia, A review on chemical coagulation/flocculation technologies for removal of colour from textile wastewaters, J. Environ. Manage. 93 (2012) 154–168.
- [2] F. Duarte, V. Morais, F.J. Maldonado-Hódar, L.M. Madeira, Treatment of textile effluents by the heterogeneous Fenton process in a continuous packed-bed reactor using Fe/activated carbon as catalyst, Chem. Eng. J. 232 (2013) 34–41.
- [3] J. Dasgupta, J. Sikder, S. Chakraborty, S. Curcio, E. Drioli, Remediation of textile effluents by membrane based treatment techniques: a state of the art review, J. Environ. Manage. 147 (2015) 55–72.
- [4] A.M. Lotito, U. Fratino, A. Mancini, G. Bergna, C. Di laconi, Effective aerobic granular sludge treatment of a real dyeing textile wastewater, Int. Biodeterior. Biodegrad. 69 (2012) 62–68.
- [5] Z. Yang, X. Liu, B. Gao, S. Zhao, Y. Wang, Q. Yue, Q. Li, Flocculation kinetics and floc characteristics of dye wastewater by polyferric chloride epoly-epichlorohydrine dimethylamine composite flocculant, Sep. Purif. Technol. 118 (2013) 583–590.
- [6] Y. Al-Ani, Y. Li, Degradation of C.I. Reactive Blue 19 using combined iron scrap process and coagulation/flocculation by a novel Al (OH)₃ epolyacrylamide hybrid polymer, J. Taiwan Inst. Chem. Eng. 43 (2012) 942–947.
- [7] G. Mezohegyi, F.P. van der Zee, J. Font, A. Fortuny, A. Fabregat, Towards advanced aqueous dye removal processes: a short review on the versatile role of activated carbon, J. Environ. Manage. 102 (2012) 148–164.
- [8] C.A. Somensi, E.L. Simionatto, S.L. Bertoli, A. Wisniewski, C.M. Radetski, Use of ozone in a pilot-scale plant for textile wastewater pre-treatment: physicochemical efficiency, degradation by-products identification and environmental toxicity of treated wastewater, J. Hazard. Mater. 175 (2010) 235–240.
- [9] S. Karthikeyan, A. Titus, A. Gnanamani, A.B. Mandal, G. Sekaran, Treatment of textile wastewater by homogeneous and heterogeneous Fenton oxidation processes, Desalination 281 (2011) 438–445.
- [10] R.-F. Yu, C.-H. Lin, H.-W. Chen, W.-P. Cheng, M.-C. Kao, Possible control approaches of the Electro-Fenton process for textile wastewater treatment using online monitoring of DO and ORP, Chem. Eng. J. 218 (2013) 341–349.
- [11] M. Punzi, B. Mattiasson, M. Jonstrup, Treatment of synthetic textile wastewater by homogeneous and heterogeneous photo-Fenton oxidation, J. Photochem. Photobiol. A 248 (2012) 30–35.
- [12] R.T. Sapkal, S.S. Shinde, M.A. Mahadik, V.S. Mohite, T.R. Waghmode, S.P. Govindwar, K.Y. Rajpure, C.H. Bhosale, Photoelectrocatalytic decolorization and degradation of textile effluent using ZnO thin films, J. Photochem. Photobiol. B 114 (2012) 102–107.
- [13] M.S. Alvarez, F. Moscoso, A. Rodríguez, M.A. Sanrom, F.J. Deive, Novel physicobiological treatment for the remediation of textile dyes-containing industrial

- effluents, Bioresour. Technol. 146 (2013) 689-695.
- [14] F. Torrades, J. García-Montaňo, Using central composite experimental design to optimize the degradation of real dye wastewater by Fenton and photo-Fenton reactions, Dyes Pigm. 100 (2014) 184–189.
- [15] A.M. Lotito, U. Fratino, G. Bergna, C. Di Iaconi, Integrated biological and ozone treatment of printing textile wastewater, Chem. Eng. J. 195–196 (2012) 261–269.
- [16] Y. Juang, E. Nurhayati, C. Huang, J.R. Pan, S. Huang, A hybrid electrochemical advanced oxidation/microfiltration system using BDD/Ti anode for acid yellow 36 dye wastewater treatment, Sep. Purif. Technol. 120 (2013) 289–295.
- [17] H. Ouni, M. Dhahbi, Removal of dyes from wastewaters using polyelectrolyte enhanced ultrafiltration, Desalin. Water Treat. 22 (2010) 355–362.
- [18] S. Barredo-Damas, M.I. Alcaina-Miranda, A. Bes-Pià, M.I. Iborra-Clar, A. Iborra-Clar, J.A. Mendoza-Roca, Ceramic membrane behavior in textile wastewater ultrafiltration, Desalination 250 (2010) 623–628.
- [19] M. Simonič, D. Vnučec, Coagulation and UF treatment of pulp and paper mill wastewater in comparison, Cent. Eur. J. Chem. 10 (2012) 127–136.
- [20] E. Alventosa-deLara, S. Barredo-Damas, M.I. Alcaina-Miranda, M.I. Iborra-Clar, Ultrafiltration technology with a ceramic membrane for reactive dye removal: optimization of membrane performance, J. Hazard. Mater. 209–210 (2012) 492–500.
- [21] N. Tahri, G. Masmoudi, E. Ellouze, A. Jrad, P. Drogui, R.B. Amar, Coupling microfiltration and nanofiltration processes for the treatment at source of dyeingcontaining effluent, J. Clean. Prod. 33 (2012) 226–235.
- [22] L. Malaeb, G.M. Ayoub, Reverse osmosis technology for water treatment: state of the art review, Desalination 267 (2011) 1–8.
- [23] W. Zuo, G. Zhang, Q. Meng, H. Zhang, Characteristics and application of multiple membrane process in plating wastewater reutilization, Desalination 222 (2008) 187–106
- [24] H. Strathmann, Electrodialysis a mature technology with a multitude of new applications, Desalination 264 (3) (2010) 268–288.
- [25] C. Huang, T. Xu, Y. Zhang, Y. Xue, G. Chen, Application of electrodialysis to the production of organic acids: state of the art and recent developments, J. Membr. Sci. 288 (2007) 1–12.
- [26] F. Ilhan, H.A. Kabuk, U. Kurt, Y. Avsar, H. Sari, M.T. Gonullu, Evaluation of treatment and recovery of leachate by bipolar membrane electrodialysis process, Chem. Eng. Process. 75 (2014) 67–74.
- [27] A. Deghles, U. Kurt, Treatment of tannery wastewater by a hybrid electrocoagulation/electrodialysis process, Chem. Eng. Prog. 104 (2016) 43–50.
- [28] S.K. Nataraj, S. Sridhar, I.N. Shaikha, D.S. Reddya, T.M. Aminabhavi, Membrane-based microfiltration/electrodialysis hybrid process for the treatment of paper industry wastewater, Sep. Purif. Technol. 57 (2007) 185–192.
- [29] C. Huang, T. Xu, Y. Zhang, Y. Xue, G. Chen, Application of electrodialysis to the production of organic acids: state of the art and recent developments, J. Membr. Sci. 288 (2007) 1–12.
- [30] K. HoChoo, C. HakLee, Membrane fouling mechanisms in the membrane-coupled anéorobic bioreactor, Water Res. 30 (1996) 1771–1780.
- [31] K. Zhang, H. Choi, M.Y. Wu, G.A. Sorial, D.D. Dionysiou, D.B. Oerther, An ecological-based analysis of irreversible membrane biofouling in MBRs, Water Sci. Technol. 55 (2007) 395–402.
- [32] Q. Wang, T. Ying, T. Jiang, D. Yang, M.M. Jahangir, Demineralization of soybean oligosaccharides extract from sweet slurry by conventional electrodialysis, J. Food Eng. 95 (2009) 410–415.
- [33] H.J. Lee, F. Sarfert, H. Strathmann, Designing of an electrodialysis desalination

- plant, Desalination 142 (2002) 267-286.
- [34] H.J. Lee, H. Strathmann, S.H. Moon, Determination of the limiting current density in electrodialysis desalination as an empirical function of linear velocity, Desalination 190 (2006) 43–50.
- [35] A. Abou-Shady, C. Peng, J. Almeria O, H. Xu, Effect of pH on separation of Pb (II) and NO₃⁻ from aqueous solutions using electrodialysis, Desalination 285 (2012) 46–53
- [36] M.C. Almecija, A. Martinez-Ferez, A. Guadix, M.P. Paez, E.M. Guadix, Influence of the cleaning temperature on the permeability of ceramic membranes, Desalination 245 (2009) 708–713.
- [37] F.J. Benitez, J.L. Acero, F.J. Real, C. Garcia, Removal of phenyl-urea herbicides in ultrapure water by ultrafiltration and nanofiltration processes, Water Res. 43 (2009) 267–276.
- [38] R. Das, C. Bhattacherjee, S. Ghosh, Effects of operating parameters and nature of fouling behavior in ultrafiltration of sesame protein hydrolysate, Desalination 237 (2009) 268–276.
- [39] Y. He, G. Li, Z. Jiang, H. Wang, J. Zhao, H. Su, Q. Huang, Diafiltration and concentration of Reactive Brilliant Blue KN-R solution by two-stage ultrafiltration process at pilot scale: technical and economic feasibility, Desalination 279 (2011) 235–242
- [40] C. Vincent-Vela, B. Cuartas-Uribe, S. Álvarez-Blanco, J. Lora-García, E. Berganti nos-Rodríguez, Analysis of ultrafiltration processes with dilatant macromolecular solutions by means of dimensionless numbers and hydrodynamic parameters, Sep. Purif. Technol. 75 (2010) 332–339.
- [41] S. Buetehorn, F. Carstensen, T. Wintgens, T. Melin, D. Volmering, K. Vossenkaul, Permeate flux decline in cross-flow microfiltration at constant pressure, Desalination 250 (2010) 985–990.
- [42] F. Waeger, T. Delhaye, W. Fuchs, The use of ceramic microfiltration and ultrafiltration membranes for particle removal from anaerobic digester effluents, Sep. Purif. Technol. 73 (2010) 271–278.
- [43] G.T. Vladisavljevic, P. Vukosavljevic, B. Bukvic, Permeate flux and fouling resistance ultrafiltration of depectinized apple juice using ceramic membrane, J. Food Eng. 60 (2003) 241–247.
- [44] R.A.R. Figueroa, A. Cassano, E. Drioli, Ultrafiltration of orange press liquor: optimization for permeate flux and fouling index by response surface methodology, Sep. Purif. Technol. 80 (2011) 1–10.
- [45] J. Xu, C.-Y. Chang, C. Gao, Performance of a ceramic ultrafiltration membrane system in pretreatment to seawater desalination, Sep. Purif. Technol. 75 (2010) 165–173.
- [46] W.X. Li, Y.J. Zhao, F. Liu, W.H. Xing, N.P. Xu, J. Shi, Theory and method of application-oriented ceramic membranes design (II) prediction of effects of membrane structure on microfiltration of particle suspension, J. Chem. Ind. Eng. (China) 54 (2003) 1290–1204
- [47] M. Ben Sik Ali, A. Mnif, B. Hamrouni, M. Dhahbi, Electrodialytic desalination of brackish water: effect of process parameters and water characteristics, Ionics 16 (2010) 621–629.
- [48] M. Ben Sik Ali, A. Mnif, B. Hamrouni, M. Dhahbi, Electrodialytic desalination of brackish water: effect of process parameters and water characteristics, Surf. Eng. Appl. Electrochem. 46 (2010) 253–262.
- [49] N. Tahri, G. Masmoudi, E. Ellouze, A. Jrad, P. Drogui, R. Ben Amar, Coupling microfiltration and nanofiltration processes for the treatment at source of dyeingcontaining effluent, J. Clean. Prod. 33 (2012) 226–235.